

A Pillararene-Based Ternary Drug-Delivery System with Photocontrolled Anticancer Drug Release

Guocan Yu, Wei Yu, Zhengwei Mao, Changyou Gao, and Feihe Huang*

In recent years, drug delivery systems (DDSs) have drawn strong attention from the chemistry and pharmacology fields.^[1] Compared with conventional anticancer medications, the crucial advantage of sophisticated DDSs is that they release the toxic drugs only when they enter the targeted tumor cells.^[2] Generally, a DDS is composed of a prodrug and a targeting unit connected by a spacer linker that can be cleaved by external stimuli, such as intracellular thiols, enzymes, light, or changes in pH.^[3] Although DDSs have undergone tremendous development to overcome the hurdles of traditional diagnosis and therapy, there still exist several issues which need to be resolved. First, the water solubility and stability of cancer drugs should be enhanced to prolong their circulation in blood compartments and target cancerous tissues, because most anticancer drugs have poor water solubility, rapid blood clearance, low tumor selectivity, and severe side effects for healthy tissues.^[4] Second, controlled release should be achieved by introducing cleavable spacer linkers, allowing the conversion of the targeted prodrug to the active drug form in the cells accurately.^[5] Third, the ability to track the process of translocation, drug release, and excretion of nanomedicine should be built into the DDSs since most of the anticancer drugs are intrinsically non-fluorescent or weakly fluorescent,^[6] such as gemcitabine and paclitaxel.

Herein, we report a supramolecular system that meets these design criteria. Specifically, a photodegradable anticancer prodrug (**Py-Cbl**) containing the anticancer drug chlorambucil and fluorophore pyrene was designed and synthesized (**Figure 1**). The photo-cleavable group here performs two important functions: (i) providing photoresponsive control over the drug release and (ii) serving as a linker between the fluorophore and the drug. Upon UV irradiation, **Py-Cbl**

is cleaved into two parts, the anticancer drug chlorambucil and 1-pyrenemethanol (**PyOH**), accompanied by significant changes in fluorescence, allowing an accurate and quantitative measurement of the drug release process. On the other hand, a water soluble pillar[6]arene (**WP6**)^[7] modified by carboxylate anionic groups on both rims first reported by our group was utilized as a supramolecular container to enhance the solubility of **Py-Cbl** mainly driven by hydrophobic interactions due to the existence of a hydrophobic cavity in the pillar structure. Moreover, a hydrophilic diblock copolymer methoxy-poly(ethylene glycol)₁₁₄-*block*-poly(L-lysine hydrochloride)₂₀₀ (PEG-*b*-PLKC) was introduced into our system to enhance the membrane permeability by PEGylation of the host-guest inclusion complex **WP6**⊃**Py-Cbl**. **WP6**⊃**Py-Cbl** acted as an anionic supramolecular cross-linker to neutralize the positively charged polylysine block through electrostatic interactions, forming stable ternary polyion complex (PIC) micelles with **WP6**⊃**Py-Cbl** and the PLKC block as the core, and the PEG block as the shell of the ternary PIC micelles.^[8] Among various external-stimuli mentioned before, light is of special interest because it can work rapidly, remotely, cleanly, and noninvasively.^[9] As discussed in detail below, this ternary supramolecular system shows off-on fluorescence changes that coincide with drug release inside the cells. It allows real-time visualization of the therapeutic response and provides useful information for dose adjustment, prognosis, and toxicity.

The absorption and emission spectra of **Py-Cbl** were first investigated by using UV and fluorescence spectroscopy. As shown in **Figure 2a** and **b**, the broad absorption band at 340 nm corresponding to **Py-Cbl** was similar to that of **PyOH** in water. However, the maximum emission band of **Py-Cbl** occurred at 500 nm, which was quite different from that of **PyOH** (400 nm). Upon irradiation with UV light for 10 min with an 8 W medium-pressure Hg lamp using a UV filter, almost no change was observed in the emission spectrum of **PyOH**. However, a distinct blue shift from 500 to 400 nm was observed in the emission spectrum for **Py-Cbl**, which became similar to that of **PyOH**, indicating the successful photodegradation of **Py-Cbl** into **PyOH** and chlorambucil. Furthermore, the cleavage of **Py-Cbl** led to a colour change of the solution from light blue to cyan (inset in **Figure 2a**). From the spectroscopic studies mentioned above, we conjectured that **Py-Cbl** could be used as a cell imaging agent to monitor the release of the anticancer drug upon UV light irradiation due to the significant changes in fluorescence.

G. Yu, Prof. F. Huang
State Key Laboratory of Chemical Engineering
Department of Chemistry
Zhejiang University
Hangzhou 310027, P. R. China
E-mail: fhuang@zju.edu.cn

W. Yu, Prof. Z. Mao, Prof. C. Gao
MOE Key Laboratory of Macromolecular Synthesis
and Functionalization
Department of Polymer Science and Engineering
Zhejiang University
Hangzhou 310027, P. R. China



DOI: 10.1002/sml.201402236

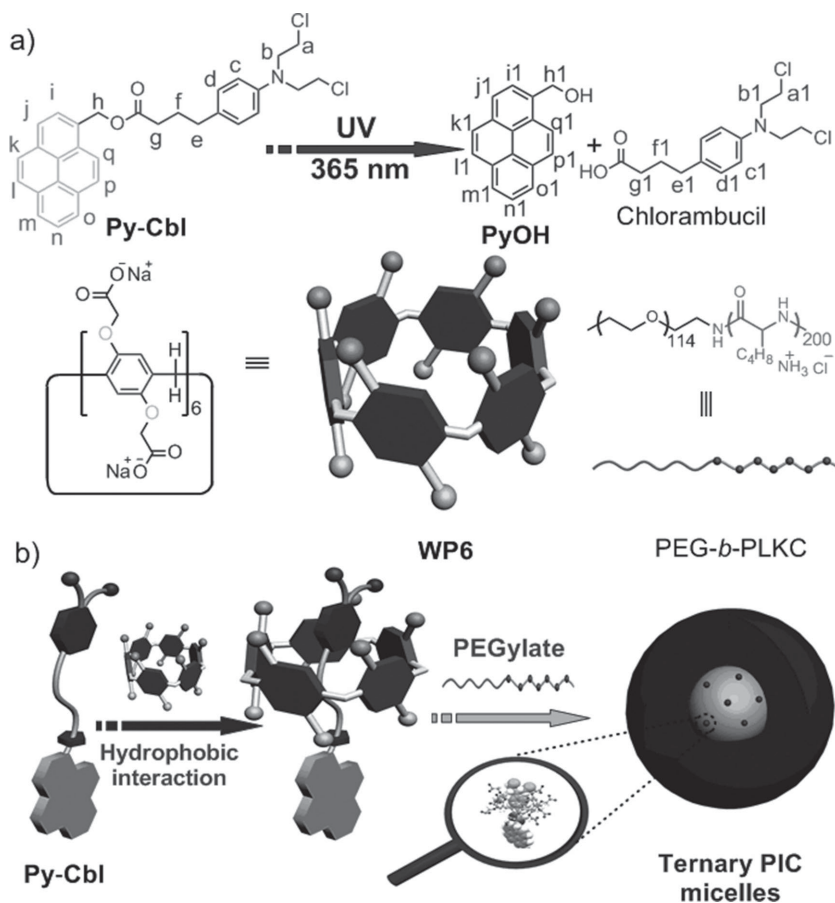


Figure 1. a) Chemical structures of **Py-Cbl**, **PyOH**, chlorambucil, **WP6** and **PEG-b-PLKC**. b) Cartoon representation of the self-assembly process of a ternary complex micelle.

Next, we utilized transmission electron microscopy (TEM) to elucidate the morphology changes of the nanostructure before and after UV irradiation. Globular nanoparticles with an average diameter of about 25 nm were observed in the TEM image (Figure 2c) of a sample prepared by slow addition of 10 μL of a dimethyl sulfoxide solution of **Py-Cbl** (3 mM) into water (20 mL) at room temperature with controlled stirring. Intriguingly, the size of the nanoparticles decreased to about 10 nm upon irradiation of the solution for 10 min (Figure 2d), which was similar to the nanoparticles formed by **PyOH** prepared under the same conditions (Figure 2e), further confirming the photodegradation of **Py-Cbl**. Dynamic light scattering (DLS) experiments provided convincing insight into the size change of the nanoparticles formed by **Py-Cbl** before and after UV irradiation. The average diameter of the nanostructures decreased from 25.7 nm to 11.6 nm upon UV irradiation for 10 min (Figure S4 and S5), in agreement with the results obtained from TEM.

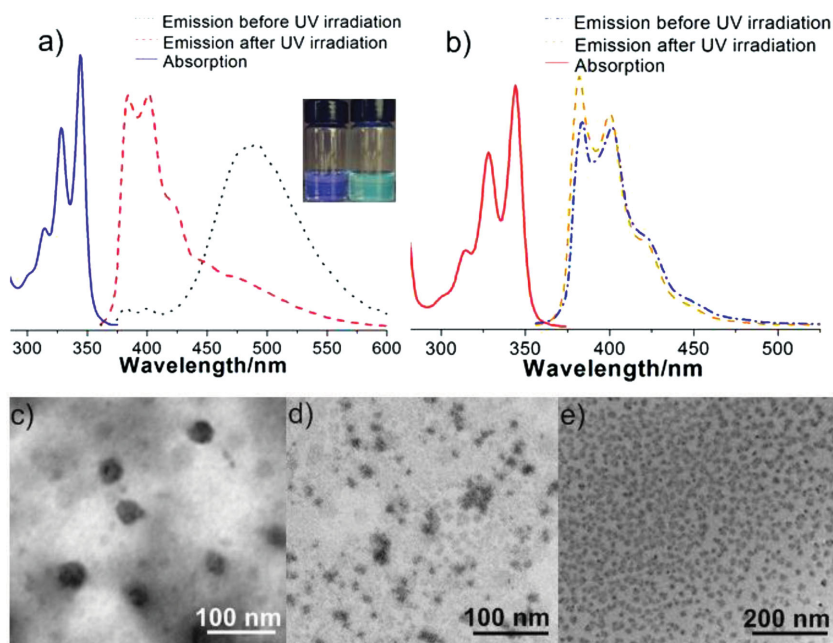


Figure 2. Normalized absorption and emission spectra of aqueous solutions: a) **Py-Cbl**, inset: colour change of the solution after irradiation with UV light for 10 min; b) 1-(hydroxymethyl) pyrene (**PyOH**). TEM images: c) **Py-Cbl** nanoparticles obtained before photolysis; d) **Py-Cbl** nanoparticles obtained after photolysis; e) **PyOH** nanoparticles.

Moreover, we chose ^1H NMR spectroscopy to monitor the gradual degradation process of **Py-Cbl**. As shown in Figure 3a, the peak related to methylene protons H^h next to pyrene diminished gradually upon UV irradiation, along with the appearance of the peak corresponding to protons H^{h1} . Similar phenomena were observed for the other peaks ($\text{H}^{a,b}$, H^e , H^d , $\text{H}^{e,g}$, H^f , and H^{i-q}) corresponding to the protons on **Py-Cbl**, confirming the occurrence of the photodegradation behaviour. The ^1H NMR spectra confirmed that **Py-Cbl** cleaved into **PyOH** and chlorambucil completely after irradiation with UV light (8 W) for 10 min (Figure 3a). It should be noted that the photodegradation process could not be achieved when **Py-Cbl** was dissolved in acetone, because water was essential for the photodegradation reaction (Figure S6).

Sophisticated methods that can effectively improve the solubilities of poorly soluble drug candidates have attracted a great deal of attention, because 40–70% of new drug candidates can not be formulated on their own arising from their poor solubilities in water.^[4c] The solubility of **Py-Cbl** in water is very poor ($<0.5 \mu\text{g/mL}$). The diameter of the internal cavity of pillar[6]arenes is $\sim 6.7 \text{ \AA}$, which is large enough to wrap up the anti-cancer prodrug **Py-Cbl**.^[9d,10] As shown

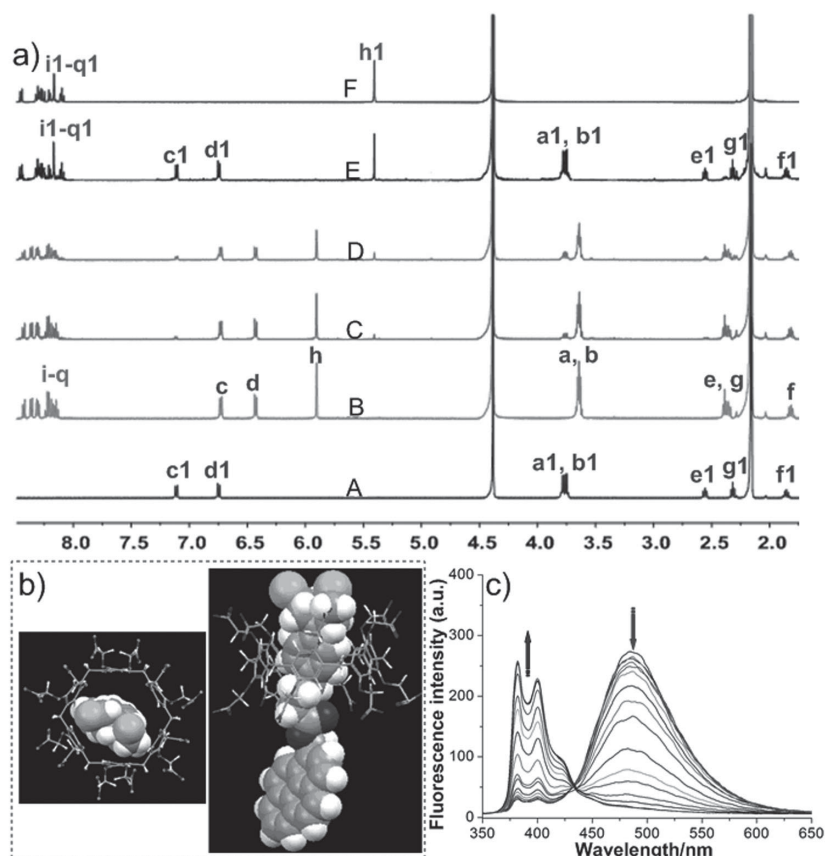


Figure 3. a) ¹H NMR spectra (500 MHz, D₂O/acetone-*d*₆ = 2:1, room temperature): A. chlorambucil; B. **Py-Cbl**; C. **Py-Cbl** after UV irradiation at 365 nm for 1 min; D. **Py-Cbl** after UV irradiation at 365 nm for 2 min; E. **Py-Cbl** after UV irradiation at 365 nm for 10 min; F. **PyOH**. b) Top and side views of the energy-minimized structure of WP6⊃Py-Cbl. c) Changes in fluorescence intensity related to WP6⊃Py-Cbl as a function of irradiation time (8 W).

in the energy-minimized structure of the host-guest complex (Figure 3b), the size of chlorambucil is suitable for the cavity of WP6 and the benzene ring on Py-Cbl can penetrate into the cavity of WP6 to form a stable inclusion complex. In order to enhance the solubility of this anticancer prodrug, WP6 possessing excellent solubility in water was utilized as a supramolecular container to encapsulate the poorly

soluble **Py-Cbl**. From fluorescent titration experiments, a substantial increase in the intensity of the emission band at 500 nm was observed upon addition of WP6 into an aqueous solution of **Py-Cbl**, which indicated that the solubility of **Py-Cbl** was enhanced by complexation with WP6 driven by hydrophobic interactions (Figure S7). The solubility of **Py-Cbl** increased gradually upon addition of WP6, and reached 58.3 μg/mL when the concentration of WP6 was 5 mM (by factors of >110 relative to the solubility of **Py-Cbl**), demonstrating that WP6 is an excellent supramolecular container to greatly enhance the solubility of the poorly soluble anticancer prodrug (Figure S9).

With the host-guest inclusion complex in hand, we studied the photodegradation rate of **Py-Cbl** in the presence of the pillar[6]arene host. Figure 3c shows the fluorescence changes of a **Py-Cbl** solution with different irradiation times. A gradual decrease in the emission band at 500 nm for **Py-Cbl** and a concomitant increase in the emission band at 400 nm were observed in the emission spectrum by increasing irradiation time, indicating gradual cleavage of **Py-Cbl**. We also employed fluorescence intensity changes to calculate the percentage of drug release upon gradual irradiation of UV light (Figure 4a and Figures S10–S14). As shown in Figure 4a, the photodegradation

rate of **Py-Cbl** decreased significantly upon addition of WP6. The time required for the complete photodegradation of **Py-Cbl** into **PyOH** and chlorambucil increased from 5 to 10 min (A and B in Figure 4a) with an 8 W medium-pressure Hg lamp, and from 13 to 18 min (C and D in Figure 4a) with a 5 W medium-pressure Hg lamp. The reason was that the ester group of **Py-Cbl** was located in the hydrophobic cavity

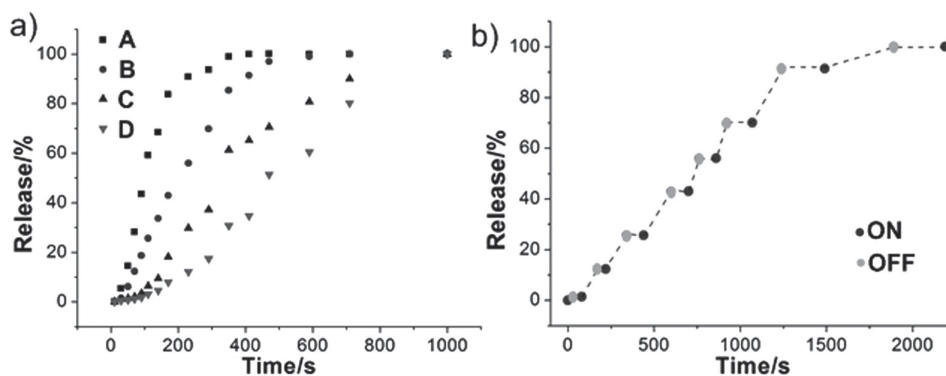


Figure 4. a) Progress of the release of chlorambucil under UV light irradiation: A. **Py-Cbl** (8 W); B. WP6⊃Py-Cbl (8 W); C. **Py-Cbl** (5 W); D. WP6⊃Py-Cbl (5 W). The concentration of **Py-Cbl** was 2.00 × 10⁻⁵ M. b) The progress of chlorambucil release after different periods of exposure to UV light and dark conditions (denoted "ON" and "OFF", respectively).

of **WP6** upon the formation of the host–guest complex as confirmed by the energy-minimized structure (Figure 3b), preventing the ester group from being hydrolyzed under UV light, resulting in the reduction of the photodegradation rate effectively. Furthermore, the precise control of the photoresponsive release of the anticancer drug was demonstrated by monitoring the fluorescence changes after different periods of exposure to UV light and dark conditions (Figure 4b), which showed that the anticancer drug release proceeded only under illumination.

The solubility problem of **Py-Cbl** was solved as demonstrated above. However, there still existed another issue to overcome before this supramolecular system could be applied as a drug delivery system. The membrane permeability of the complex containing the anticancer drug should be improved, because the anionic host–guest complex was hardly able to penetrate the cell membrane mainly comprised of a phospholipid bilayer. Poly(ethylene glycol) (PEG), one of the most common non-ionic bioacceptable and nontoxic hydrophilic polymers, has been used in a wide variety of established and emerging applications in pharmaceuticals.^[11] Nanostructures coated with PEG can form “brushlike” structures, preventing proteins from penetrating the substrate surface and shielding secondary adsorption onto the outer surface.^[11b] Moreover, it decreases the aggregation tendency of particles through steric stabilization and is often used to improve the biocompatibility of various systems to prolong blood circulation times, increasing the probability that the drug reaches its site of action before being recognized as foreign and cleared from the body.

PEG-*b*-PLKC was chosen to PEGylate the anionic inclusion complex **WP6**⊃**Py-Cbl**, which could serve as an anionic supramolecular cross-linker to connect the positively charged polylysine segments driven by electrostatic interactions, forming a polymeric supramolecular amphiphile in aqueous solution.^[12] Stable ternary PIC micelles were obtained with **WP6**⊃**Py-Cbl** and the PLKC block as the core and the PEG block as the shell.^[12b] In this ternary system, the ratio *r* between positive and negative charges played a significant role in the formation and stability of the aggregates. DLS was utilized to monitor the self-assembly of the solution with different *r* values. As shown in Figure S15a, the DLS count rate depended strongly on the *r* at constant concentration of PEG-*b*-PLKC. The count rate of the sample increased gradually as the *r* value changed from 1:10 to 1:1, indicating the effective formation of the ternary complex.^[12b] Further addition of anionic **WP6**⊃**Py-Cbl** resulted in a slight decrease of the count rate as the neutral state of the core changed into the hydrophilic negatively charged state upon addition of excess anionic component, resulting in disturbing the self-assembly of PEG-*b*-PLKC and **WP6**⊃**Py-Cbl** to some extent. The optimal *r* value of the ternary system was obtained to be 1:1, demonstrating that complete complexation was achieved when the core of the complex was in the neutral state.

TEM and fluorescence microscopy were employed to reveal the morphology of the ternary complex (*r* = 1:1). As shown in Figure S15b, spherical aggregates were observed with the diameters ranging from 80 to 160 nm. Notably, no sharp color contrast between the periphery and central parts

was found, suggesting that the spherical nanostructures were micelles. On the other hand, fluorescence microscopy was used to verify the structure of the ternary complex due to the existence of the fluorescent chromophore in **Py-Cbl**. As indicated by the fluorescence microscopic image (Figure S15c), spherical nanostructures were observed, confirming the result obtained by TEM. Furthermore, the average size of the aggregates was 127 nm indicated by DLS in Figure S15d, in good agreement with the results obtained from TEM and fluorescence microscopy. It should be noted that the PIC micelles formed from PEG-*b*-PLKC and **WP6**⊃**Py-Cbl** were quite stable in buffer for several weeks without structural changes. The stability of the PEGylated ternary PIC micelles containing the anticancer prodrug was improved effectively, accompanied by improvement of the membrane permeability of this ternary supramolecular system.

Nanosized vehicles including peptides, liposomes, dendrimers, vesicles, polymer nanoparticles, and some inorganic materials have been utilized as the nanocarriers of the drugs to effectively enhance their water solubility and stability, thus prolonging their circulation in blood compartments, target cancerous tissues through the enhanced permeation and retention (EPR) effect.^[13] However, it is hard to visualize these drug delivery processes because most of the anticancer drugs, such as gemcitabine, paclitaxel, are intrinsically non-fluorescent or weakly fluorescent. Therefore, tracking the process of drug release and nanomedicine excretion is of critical importance. By introducing a fluorophore into the DDSs, an accurate and quantitative measurement of drug release process can be achieved.

To demonstrate that this ternary complex could be employed as a versatile DDS, initial cell imaging studies were carried out using an A549 cell line. A cellular uptake study after 24 h incubation of A549 cells with the ternary PIC micelles revealed that the PIC micelles were internalized by the cell membrane, leading to a uniform distribution in cytoplasm (Figure 5a and b). As discussed above, notable changes in spectroscopic behavior and colour were monitored upon irradiation of UV light due to the photodegradation of **Py-Cbl**, accompanied by the release of chlorambucil. This was employed to monitor the drug release in the cell in real time using the fluorescence imaging technique. The colour of the cells changed from bright blue (Figure 5b) to dark blue (Figure 5d) due to the photodegradation of **Py-Cbl** into **PyOH** and chlorambucil, consistent with the results mentioned in Figure 2a.

Controllable release of anticancer drug *in vitro* was verified by using the MTT [MTT = 3-(4',5'-dimethylthiazol-2'-yl)-2,5-diphenyltetrazolium bromide] assay on the A549 cell line. The cytotoxic effect of each treatment was expressed as the percentage of cell viability relative to the untreated control cells. MTT assays were performed by exposing the cells to **Py-Cbl**, **WP6**⊃**Py-Cbl**, the ternary PIC micelles, and chlorambucil, respectively, with concentrations ranging from 10 to 50 μM. As shown in Figure 5e, relative cell viability of A549 cells cultured with **Py-Cbl**, **WP6**⊃**Py-Cbl** and the ternary PIC micelles showed minimal influence on cell viability and proliferation in a concentration range of up to 50 μM, indicating

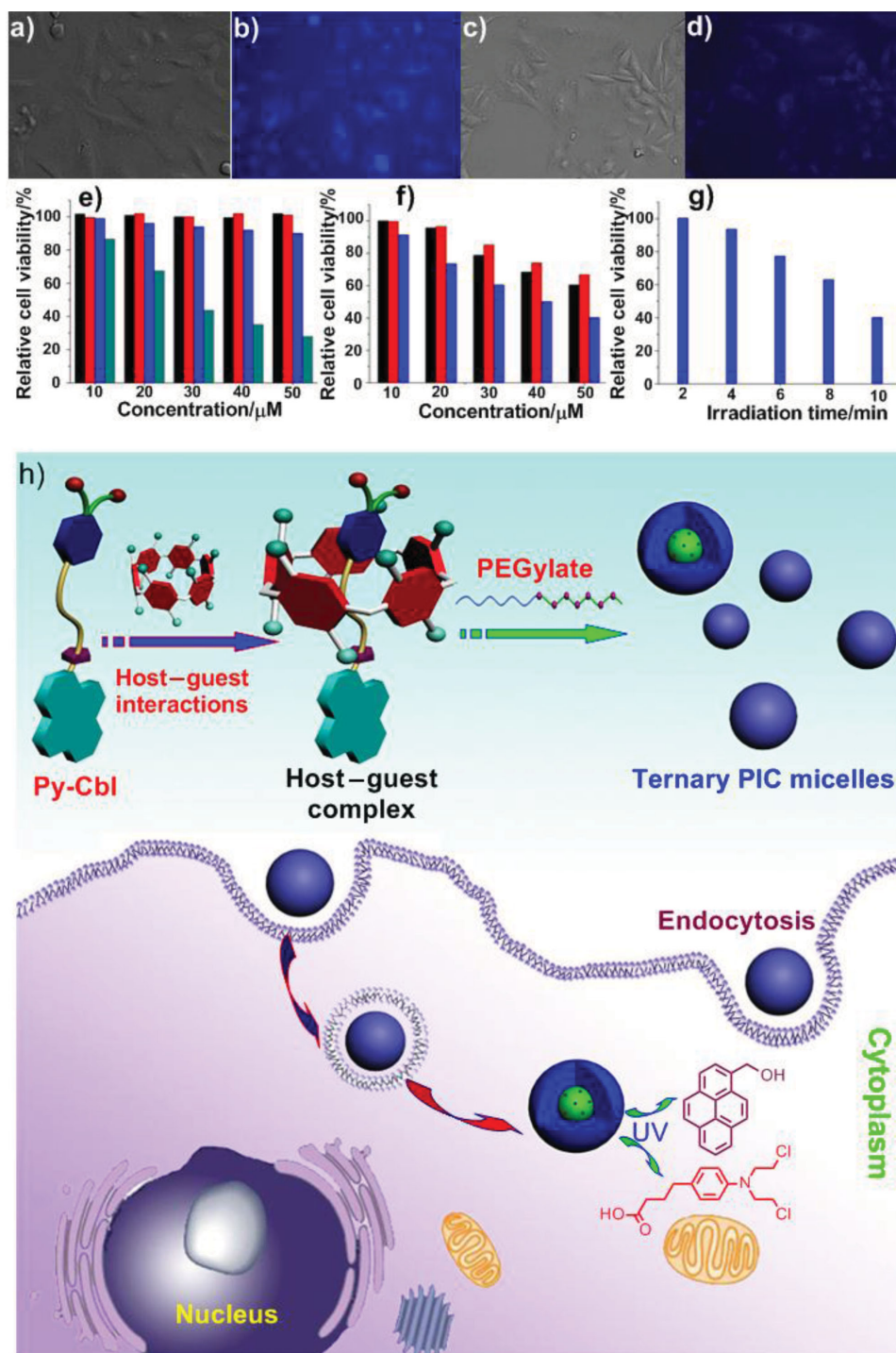


Figure 5. Real-time drug release studies using fluorescence microscopy: a) bright field image of A549 cells incubated with **Py-Cbl** before UV light irradiation; b) fluorescence image of a); c) bright field image of A549 cells incubated with **Py-Cbl** after UV light irradiation for 10 min; d) fluorescence image of c). e) Cell viability tests of **Py-Cbl** (black column), **WP6 \rightarrow Py-Cbl** (red column), ternary complex (blue column), and chlorambucil (cyan column) against A549 cells. f) Cell viability tests of A549 cell line in the presence of different concentrations of **Py-Cbl** (black column), **WP6 \rightarrow Py-Cbl** (red column) and ternary complex (blue column) after UV irradiation for 10 min. g) Cell viability tests of A549 cell line in the presence of the ternary complex after UV irradiation for different times. The concentration of **Py-Cbl** was 5×10^{-5} M. h) Schematic illustration of the preparation of ternary PIC micelles and possible cellular pathways. The ternary PIC micelles are endocytosed by cancer cells and chlorambucil is released upon UV irradiation.

low toxicity. On the contrary, the relative cell viability of the cells incubated with chlorambucil decreased gradually from 86.7% to 27.8% from 10 to 50 μM , confirming high cytotoxicity of this anticancer drug. The results obtained

from MTT experiments demonstrated that the toxicity was decreased significantly by introducing the photoresponsive fluorophore onto the drug to form the prodrug, effectively reducing side effects to healthy tissue.

More importantly, the photodegradation of **Py-Cbl** can be regulated easily upon irradiation of UV light, resulting in the achievement of controllable anticancer drug release. Irradiation for 10 min under UV light (365 nm) resulted in the release of chlorambucil for the cells cultured with **Py-Cbl**, **WP6**⊃**Py-Cbl** and the ternary PIC micelles that all contained photodegradable **Py-Cbl**, thereby causing cytotoxicity to the cancerous A549 cell lines, as verified by the MTT toxicity data shown in Figure 5f. The toxicity here could be used to determine the cellular uptake amount of **Py-Cbl**, because the more drug the cells took, the higher the toxicity exhibited due to complete release of chlorambucil upon UV light irradiation for enough time (10 min as proved in Figure 3). Among these three systems, the ternary PIC micelles showed the highest cytotoxicity, followed by **Py-Cbl**, with **WP6**⊃**Py-Cbl** showing the lowest cytotoxicity (Figure 5f), indicating that the cellular uptake amount of these three systems was that: ternary PIC micelles >**Py-Cbl** >**WP6**⊃**Py-Cbl**. The cellular uptake of **Py-Cbl** was also validated by UV-vis spectroscopy (Figure S16). Notably, the cellular absorption intensity of solutions of ternary PIC micelles was higher than that of **Py-Cbl**, and the cellular absorption intensity of **WP6**⊃**Py-Cbl** solution was the lowest among these three groups under the same conditions, in accord with the results obtained from the MTT data. The membrane permeability of **Py-Cbl** was better than that of **WP6**⊃**Py-Cbl**, because the anionic host-guest inclusion complex **WP6**⊃**Py-Cbl** could not easily penetrate the cell membrane. Compared with **WP6**⊃**Py-Cbl**, **Py-Cbl** self-assembled into nanoparticles with diameter about 25 nm displayed better biocompatibility and cellular uptake, resulting in the exhibition of higher toxicity after complete release of chlorambucil by UV irradiation. Upon formation of ternary PIC micelles by supramolecular modification, the membrane permeability of the micelles was enhanced significantly. In comparison with **Py-Cbl** and **WP6**⊃**Py-Cbl** at the same concentration, more PIC micelles containing the anticancer prodrug were taken up by the cells, thus attaining the highest level of toxicity (about 59.7% in comparison to the control).

As demonstrated above, drug loading was enhanced strongly by using **WP6** as a supramolecular container mainly driven by hydrophobic interactions. On the other hand, the biocompatibility and membrane permeability of the host-guest inclusion complexes were improved by forming ternary PIC micelles with PEG as the shell. Furthermore, in order to verify the ability of ternary PIC micelles containing anticancer prodrugs to be used for externally regulated drug release, A549 cells cultured with the ternary PIC micelles were exposed to UV light for different time intervals. As shown in Figure 5g, the cytotoxicity toward A549 cells clearly increased by increasing irradiation time, indicating that the amount of the drug released from the ternary PIC micelles can be adjusted by controlling the irradiation time. Possible cellular pathways were illustrated in Figure 5h. The ternary PIC micelles entered the cytoplasm through endocytosis. Upon UV irradiation, the anticancer drug was released from the micelles inside the cells *via* photodegradation of **Py-Cbl** into **PyOH** and chlorambucil, accompanied by a colour change of the cells. In our system, we could irradiate

the tumor tissue by UV light, allowing the conversion of the anticancer prodrug **Py-Cbl** into the active drug form in the tumor cells accurately, which endowed the ternary PIC micelles with targeting anticancer capability.

In summary, a novel photodegradable anticancer prodrug (**Py-Cbl**) containing chlorambucil and a fluorophore pyrene moiety was designed and synthesized. In order to enhance the solubility of **Py-Cbl**, a water soluble pillar[6]arene (**WP6**) was utilized as a supramolecular container to wrap up the anticancer drug via hydrophobic interactions. Due to the formation of a stable host-guest inclusion complex between **WP6** and **Py-Cbl**, the photodegradation rate of the drug was slowed. On the other hand, the release of chlorambucil could be controlled easily by UV irradiation. To improve the membrane permeability of **WP6**⊃**Py-Cbl**, the diblock polymer PEG-*b*-PLKC was employed to form stable ternary polyion complex (PIC) micelles with **WP6**⊃**Py-Cbl** and the polylysine segment as the core and the PEG block as the shell. By introducing the non-ionic, bioacceptable and nontoxic hydrophilic PEG into this supramolecular system, the biocompatibility and membrane permeability of the ternary PIC micelles were enhanced significantly. Compared with chlorambucil, the cytotoxicity of **Py-Cbl** was decreased effectively by introducing the fluorescent chromophore pyrene as confirmed by MTT assays. Furthermore, the changes in the fluorescence were utilized to indicate loading and unloading of the drug upon photodegradation of **Py-Cbl** into **PyOH** and chlorambucil. This system successfully addressed three key issues: 1) enhancement of the water solubility of the anticancer prodrug; 2) controlled release of the anticancer drug; 3) accurate and quantitative measurement of the drug release. Such ternary supramolecular system may open up new perspectives for designing a new class of promising stimuli-responsive nanocarriers for drug delivery.

Supporting Information

Supporting Information is available from the Wiley Online Library or from the author.

Acknowledgements

This work was supported by National Basic Research Program (2013CB834502), the National Natural Science Foundation of China (21125417), and the Fundamental Research Funds for the Central Universities.

- [1] a) N. K. Mal, M. Fujiwara, Y. Tanaka, *Nature* **2003**, *421*, 350; b) S. S. Agasti, A. Chompoosor, C. You, P. Ghosh, C. K. Kim, V. M. Rotello, *J. Am. Chem. Soc.* **2009**, *131*, 5728; c) Z. Luo, K. Cai, Y. Hu, J. Li, X. Ding, B. Zhang, D. Xu, W. Yang, P. Liu, *Adv. Mater.* **2012**, *24*, 431; d) C. Li, S. Liu, *Chem. Commun.* **2012**, *48*, 3262.
[2] a) M. Shi, J. Lu, M. S. Shoichet, *J. Mater. Chem.* **2009**, *19*, 5485; b) S. D. Brown, P. Nativo, J.-A. Smith, D. Stirling, P. R. Edwards,

- B. Venugopal, D. J. Flint, J. A. Plumb, D. Graham, N. J. Wheate, *J. Am. Chem. Soc.* **2010**, *132*, 4678; c) Y. Namiki, T. Fuchigami, N. Tada, R. Kawamura, S. Matsunuma, Y. Kitamoto, M. Nakagawa, *Acc. Chem. Res.* **2011**, *44*, 1080; d) M. J. Sailor, J.-H. Park, *Adv. Mater.* **2012**, *24*, 3779; e) J. Li, Z. Ge, S. Liu, *Chem. Commun.* **2013**, *49*, 6974.
- [3] a) D. A. Edwards, J. Hanes, G. Caponetti, J. Hrkach, A. Ben-Jebria, M. L. Eskew, J. Mintzes, D. Deaver, N. Lotan, R. Langer, *Science* **1997**, *276*, 1868; b) C. Park, J. Lim, M. Yun, C. Kim, *Angew. Chem. Int. Ed.* **2008**, *47*, 2959; c) A. Jana, K. S. P. Devi, T. K. Maiti, N. D. P. Singh, *J. Am. Chem. Soc.* **2012**, *134*, 7656; d) S. A. Mackowiak, A. Schmidt, V. Weiss, C. Argyo, C. Schirnding, T. Bein, C. Brauchle, *Nano Lett.* **2013**, *13*, 2576; e) Z. Ge, S. Liu, *Chem. Soc. Rev.* **2013**, *42*, 7289; f) M. H. Lee, Z. Yang, C. W. Lim, Y. H. Lee, S. Dongbang, C. Kang, J. S. Kim, *Chem. Rev.* **2013**, *113*, 5071.
- [4] a) M. V. Rekharsky, Y. Inoue, *Chem. Rev.* **1998**, *98*, 1875; b) V. J. Stella, K. W. Nti-Addae, *Adv. Drug Deliv. Rev.* **2007**, *59*, 677; c) D. Ma, G. Hettiarachchi, D. Nguyen, B. Zhang, J. B. Wittenberg, P. Y. Zavalij, V. Briken, L. Isaacs, *Nature Chem.* **2012**, *4*, 503; d) T. Minami, N. A. Esipenko, B. Zhang, L. Isaacs, R. Nishiyabu, Y. Kubo, P. Anzenbacher Jr., *J. Am. Chem. Soc.* **2012**, *134*, 20021.
- [5] a) S. Simovic, D. Losic, K. Vasilev, *Chem. Commun.* **2010**, *46*, 1317; b) M. A. Yassin, D. Appelhans, R. G. Mendes, M. H. Rummeli, B. Voit, *Chem. Eur. J.* **2012**, *18*, 12227; c) H. Meng, W. X. Mai, H. Zhang, M. Xue, T. Xia, S. Lin, X. Wang, Y. Zhao, Z. Ji, J. I. Zink, A. E. Nel, *ACS Nano* **2013**, *7*, 994; d) M. L. Viger, M. Grossman, N. Fomina, A. Almutairi, *Adv. Mater.* **2013**, *25*, 3733.
- [6] a) Y. Gu, Y. Zhong, F. Meng, R. Cheng, C. Deng, Z. Zhong, *Biomacromolecules* **2013**, *14*, 2772; b) G. Y. Lee, W. Pan, L. Wang, Y. A. Wang, C. A. Staley, M. Satapathy, S. Nie, H. Mao, L. Yang, *ACS Nano* **2013**, *7*, 2078; c) S. Bhuniya, S. Maiti, E.-J. Kim, H. Lee, J. L. Sessler, K. S. Hong, J. S. Kim, *Angew. Chem. Int. Ed.* **2014**, *53*, 4469–4474.
- [7] a) G. Yu, M. Xue, Z. Zhang, J. Li, C. Han, F. Huang, *J. Am. Chem. Soc.* **2012**, *134*, 13248; b) G. Yu, X. Zhou, Z. Zhang, C. Han, Z. Mao, C. Gao, F. Huang, *J. Am. Chem. Soc.* **2012**, *134*, 19489.
- [8] a) Y. Lee, T. Ishii, H. J. Kim, N. Nishiyama, Y. Hayakawa, K. Itaka, K. Kataoka, *Angew. Chem. Int. Ed.* **2010**, *49*, 2552; b) C. Wang, Q. Chen, Z. Wang, X. Zhang, *Angew. Chem. Int. Ed.* **2010**, *49*, 8612.
- [9] a) B. Yan, J.-C. Boyer, N. R. Branda, Y. Zhao, *J. Am. Chem. Soc.* **2011**, *133*, 19714; b) M. P. Melancon, M. Zhou, C. Li, *Acc. Chem. Res.* **2011**, *44*, 947; c) G. Yu, C. Han, Z. Zhang, J. Chen, X. Yan, B. Zheng, S. Liu, F. Huang, *J. Am. Chem. Soc.* **2012**, *134*, 8711.
- [10] a) C. Han, Z. Zhang, X. Chi, M. Zhang, G. Yu, F. Huang, *Acta Chim. Sinica* **2012**, *70*, 1775; b) C. Han, L. Gao, G. Yu, Z. Zhang, S. Dong, F. Huang, *Eur. J. Org. Chem.* **2013**, 2529.
- [11] a) K. Y. Choi, H. Y. Yoon, J.-H. Kim, S. M. Bae, R.-W. Park, Y. M. Kang, I.-S. Kim, I. C. Kwon, K. Choi, S. Y. Jeong, K. Kim, J. H. Park, *ACS Nano* **2011**, *5*, 8591; b) J. M. Fuller, K. R. Raghupathi, R. R. Ramireddy, A. V. Subrahmanyam, V. Yesilyurt, S. Thayumanavan, *J. Am. Chem. Soc.* **2013**, *135*, 8947.
- [12] a) Y. Lee, K. Miyata, M. Oba, T. Ishii, S. Fukushima, M. Han, H. Koyama, N. Nishiyama, K. Kataoka, *Angew. Chem. Int. Ed.* **2008**, *47*, 5163–5166; b) C. Wang, Y. Kang, K. Liu, Z. Li, Z. Wang, X. Zhang, *Polym. Chem.* **2012**, *3*, 3056.
- [13] a) C. C. Lee, J. A. MacKay, J. M. J. Frechet, F. C. Szoka, *Nat. Biotechnol.* **2005**, *23*, 1517; b) P. Horcajada, C. Serre, G. Maurin, N. A. Ramsahye, F. Balas, M. Vallet-Regi, M. Sebban, F. Taulelle, G. Ferey, *J. Am. Chem. Soc.* **2008**, *130*, 6774; c) M. P. Borgman, A. Ray, R. B. Kolhatkar, E. A. Sausville, A. M. Burger, H. Ghandehari, *Pharm. Res.* **2009**, *26*, 1407; d) M. E. Fox, F. C. Szoka, J. M. J. Frechet, *Acc. Chem. Res.* **2009**, *42*, 1141; e) E. Soussan, S. Cassel, M. Blanzat, I. Rico-Lattes, *Angew. Chem. Int. Ed.* **2009**, *48*, 274.

Received: July 26, 2014
Revised: August 26, 2014
Published online: October 15, 2014